# Interlinked roles for HEB and Id3 in fetal gamma-delta T cell commitment and functional programming

Johanna S. Selvaratnam[1,2], Juliana Dutra Barbosa da Rocha[1,2], Vinothkumar Rajan[1,2], Helen Wang[1,2], Emily C. Reddy[3], Miki S. Gams[2,3], Cornelis Murre[4], Cynthia J. Guidos[2,3], Juan Carlos Zúñiga-Pflücker[1,2], Michele K. Anderson[1,2]*

**Affiliations:**

[1]Biological Sciences, Sunnybrook Research Hospital, Toronto, ON, Canada

[2]Department of Immunology, University of Toronto, Toronto, ON, Canada

[3]Hospital for Sick Children, Toronto, ON, Canada

[4]Department of Molecular Biology, University of California at San Diego, La Jolla, CA 92093, USA

*Corresponding author: manderso@sri.utoronto.ca

Definitions of Acyronyms: TCR, T cell receptor; Id, Inhibitor of DNA binding; HEB, HeLa binding box transcription factor; IL, interleukin; E, embryonic day; V, variable region; Egr, early growth response; DP, $CD4^+CD8^+$ double positive thymocytes; DN, $CD4^-CD8^-$ double negative thymocytes; UMAP, uniform manifold approximation and projection for dimensional reduction, PCA, principle component analysis; sc, single cell

**ABSTRACT**

γδ T cells that produce IL-17 (γδT17) play essential roles in barrier immunity, but the gene networks that install their functions are not well understood. We previously linked T cell receptor (TCR) signal strength to the proportional upregulation of *Id3* during T cell development, which antagonizes the activity of HEB (encoded by *Tcf12*), and showed that HEB is required for γδT17 development. To understand how HEB and Id3 regulate γδT17 cell development, we conducted single cell RNA-sequencing on fetal thymic γδ T cells from *Tcf12*-deficient mice. γδ T cells lacking HEB exhibited profound alterations in the expression of the genes encoding the TCRγ and TCRδ chains, accompanied by a decrease in expression of genes in the early γδ T cell specification network. Surprisingly, *Id3* was among the most severely decreased genes in HEB-deficient γδ T cell precursors, suggesting a requirement for HEB in *Id3* expression. Analysis of fetal thymic γδ T cells in *Id3*-deficient mice revealed that the TCRγ and TCRδ repertoires were unaffected, and expression of early γδ T cell genes was unperturbed. However, later stage regulators of γδT17 cell differentiation were decreased, and *Id3*-deficient γδ T cells were defective in IL-17 production. Therefore, our findings reveal an interlinked network in which HEB is initially required to upregulate *Id3* expression, which in turn enables the later stages of γδT17 cell development and functional programming.

**One Sentence Summary:** During γδ T cell development, the transcription factor HEB upregulates its antagonist Id3, which is required in turn for the maturation of pro-inflammatory γδ T cells.

## INTRODUCTION

IL-17 producing γδ T cells (γδT17) are critical mediators of immunity to bacterial and fungal pathogens, and also participate in maintaining barrier integrity, particularly in mucosal tissues including the skin, gut, lungs, and female reproductive tract (*1-3*) . However, dysregulation of γδT17 cells also can induce or foster serious adverse outcomes, including autoimmune diseases such as psoriasis, multiple sclerosis, and diabetes (*4, 5*). γδT17 cells also reside in the meninges and play an important role in stress-induced depression (*6*), as well as exacerbating tumor growth and metastasis (*7, 8*). γδ T cells also play critical roles in adipose tissue homeostasis and temperature regulation (*9*), underscoring their broad clinical importance. Thus, understanding how γδT17 cells acquire their functional properties during development will enable manipulation of these functions, providing new approaches for diagnosis and treatment of multiple health conditions and diseases.

As T cells develop in the thymus from hematopoietic stem cells, a series of differentiation intermediates arise that set the stage for subsequent branchpoints and T-lineage fate choices. One of the earliest branchpoints during T cell development is the bifurcation of progenitor T (pro-T) cells into the αβ or the γδ T cell lineage (*10*). Following T cell receptor (TCR) rearrangements, committed γδ-T cell precursors differentiate into distinct functional subsets. T cell development progresses through different stages described by the "cocktail party" paradigm, wherein groups of partygoers interact and then move on to form different conversational clusters, with new participants arriving and departing as the evening progresses (*11*). The participants and their interactions have been well characterized in the αβ-T lineage fate choices, with a clear role for TCR signaling in directing dispersal and re-grouping of transcriptional regulators (*12-14*). By

contrast, much less is known about the transcriptional hand-offs that occur during γδ T cell development.

γδ T cells play key roles in mediating barrier integrity and immunity by rapid production of pro-inflammatory cytokines and/or growth factors that promote tissue homeostasis (*15-18*). In mice, different subsets of γδ T cells are specialized by distinct developmental pathways and effector functions that are tightly linked with the expression of specific Vγ and Vδ chains. In the adult thymus, the majority of γδ T cells express Vγ4 or Vγ1, paired with heterogeneous Vδ chains. After intrathymic development, γδ T cells exit the thymus as interferon-γ (IFNγ) producers (γδT1) or as naïve γδ T cells that can be polarized in the periphery (*19-21*). Specialized IL-4 producing Vγ1 Vδ6.3 γδ T cells also develop in the early postnatal thymus (*22, 23*). Vγ7 cells develop neonatally in a thymic independent manner and reside in the intestinal epithelium (*24*). Very few Vγ7 cells are detectable in the fetal thymus (*25-27*).

γδ T cells that arise within the fetal thymus appear in transient waves of development that are reflective of the order of Vγ and Vδ rearrangement during ontogeny (*28-32*). There are two nomenclature systems for Vγ and Vδ elements, here we use the Tonegawa nomenclature (*33*). At E15-E17, Vγ5 Vδ1 bearing γδ T cells develop in the thymus and then migrate to the skin where they reside for life (*18, 25, 34*). This is followed by the appearance of Vγ6 Vδ1 T cells at E16-18, and then Vγ4 Vδ5 T cells at E18-20. These cells can give rise to IL-17 producing γδ T cells (γδT17) that are most prominent and protective in barrier tissues, such as the dermis, intestinal lamina propria, lung, reproductive tract, meninges, and gingiva (*1-3*). Since the underlying gene networks that control γδ T cell functional programming are highly conserved between mice and humans (*35-37*), insights gained from mouse models are highly relevant to human T cell biology.

The linkage between γδTCR chains and functional programming stems from two main factors. Upstream of the TCR signal, there is coordinated programming of rearrangement of specific Vγ and Vδ chains (*38, 39*). Subsequently, TCR ligand engagement and downstream signaling pathways provide instructive input into γδ T cell fate and function (*10, 40-42*). In T cell precursors, weak pre-TCR (pTα/TCRβ) signaling specifies the αβ-fate (β-selection), whereas stronger γδTCR signaling drives cells into the γδ T cell lineage (γδ-selection) (*43-45*). Immature, committed fetal γδ T cells then go through a second differentiation step that subdivides them into the γδT1 or γδT17 lineages (*39, 41*). Strong signaling through the Vγ5 Vδ1 TCR, marked by upregulation of CD73, leads to the γδT1 fate during the first wave, whereas intermediate signaling through the Vγ4 Vδ5 TCR promotes differentiation into the γδT17 fate in the third wave just prior to birth (*28, 46-49*). Maturation of both lineages is accompanied by downregulation of CD24 expression. There is conflicting evidence on the strength of signal needed to select and program Vγ6 Vδ1 T cells into the γδT17 lineage during the second wave (*47, 50, 51*). Additionally, the molecular connections between TCR signal strength and expression of the genes needed for functionality are not well understood.

The E protein transcription factors HEB (*Tcf12*) and E2A (*Tcf3*) are important regulators of T-lineage gene expression throughout development, with shifting target genes in different developmental subsets (*52-55*). E protein activity is controlled by Id proteins, which sequester them into inactive dimers incapable of binding DNA (*56*). *Id3* is upregulated by TCR signaling through the ERK-Egr pathway (*57-59*). Moreover, *Id3* is upregulated proportionally to TCR signal strength, suggesting that titration of E protein activity is a key determinant of fate choice downstream of TCR signaling (*48, 59-61*). We have shown that HEB is required for γδT17 cell

development and that forced *Id3* expression in γδ T cell precursors reduced expression of several key γδ T cell regulators (*27*). HEB is also important for the later stages of αβ T cell development in the adult thymus, particularly at the immature CD8 single positive (ISP) to double positive ($CD4^+CD8^+$; DP) transition and for maturation of CD4 single positive thymocytes (*55, 62*). Thus, the E/Id protein axis connects TCR signal strength and fate-determining gene expression networks during T cell development.

To elucidate how HEB and Id3 regulate γδ T cell development, we compared γδ T cells from the fetal thymuses of $HEB^{fl/fl:Vav\text{-}iCre}$ (HEB conditionally deficient, HEB cKO) mice, *Id3*-deficient (Id3-KO) mice, and wildtype (WT) mice. Our results revealed several layers of dysregulation in the absence of HEB, including major changes in Vγ and Vδ gene expression and a dramatic decrease in the expression of early developmental regulators. We also found that HEB is required for the upregulation of *Id3* in early γδT17 cell precursors, and that Id3 is needed for effective γδT17 cell maturation. Taken together, our results indicate that HEB induces first stage γδ T cell regulators and simultaneously launches γδT17 differentiation through an Id3-mediated negative feedback loop that switches programs from HEB-dependent gene expression to the expression of genes that require Id3 mediated suppression of E protein activity.

## RESULTS

### Alterations in γδ T cell development in the HEB cKO fetal thymus

To understand the impacts of HEB deficiency on fetal γδ T cell development, we performed timed matings of HEB$^{fl/fl}$ mice (WT) with HEB$^{fl/fl}$ Vav-iCre transgenic (HEB cKO) mice to yield WT (Vav-iCre$^{-}$) and HEB cKO (Vav-iCre$^{+}$) littermates. Fetal thymuses were harvested at embryonic day 18 (E18), and thymocytes were analyzed by flow cytometry. We observed a decrease in total thymic cellularity (**Fig. 1A**), and a severe arrest in development at the immature CD8 to double positive (DP; CD4$^{+}$CD8$^{+}$) transition (**Fig. S1**), consistent with the previously reported phenotype in adult and neonatal HEB-deficient mice (*62, 63*). Although the proportion of γδ T cells among all thymocytes was higher in HEB cKO fetal thymus than in WT mice (**Fig. 1B, C**), the absolute numbers of γδ T cells were similar (**Fig. 1D**). Within the γδ T cell population, there was a severe decrease in both the percentages and the absolute cell numbers of Vγ4 cells in HEB cKO mice and a corresponding increase in the percentages and absolute cell numbers in all other Vγ subsets (**Fig.1E-G**). Nearly all Vγ4 cells were immature, as assessed by high CD24 expression, in both WT and HEB cKO mice (**Fig. 1H, I**). However, Vγ5, Vγ1, and Vγ4$^{-}$5$^{-}$1$^{-}$ T cell subsets had higher percentages of CD24$^{+}$ immature γδ T cells in the HEB cKO mice relative to WT mice (**Fig. 1H-K**), suggesting a partial block or delay in maturation. As Vγ6 cells CD3$^{high}$ relative to other Vγ subsets (*64*), the high levels of CD3 on Vγ4$^{-}$5$^{-}$1$^{-}$ cells indicated that these were primarily Vγ6 cells (**Fig. 1J**). Furthermore, Vγ7 cells are scarce in the fetal thymus (*27*). Therefore, for simplicity, we will refer to Vγ4$^{-}$5$^{-}$1$^{-}$ cells as Vγ6 cells in our flow cytometry data. These findings indicate a lack of HEB results in the depletion of Vγ4 cells and an impairment in γδ T cell maturation in the fetal thymus.

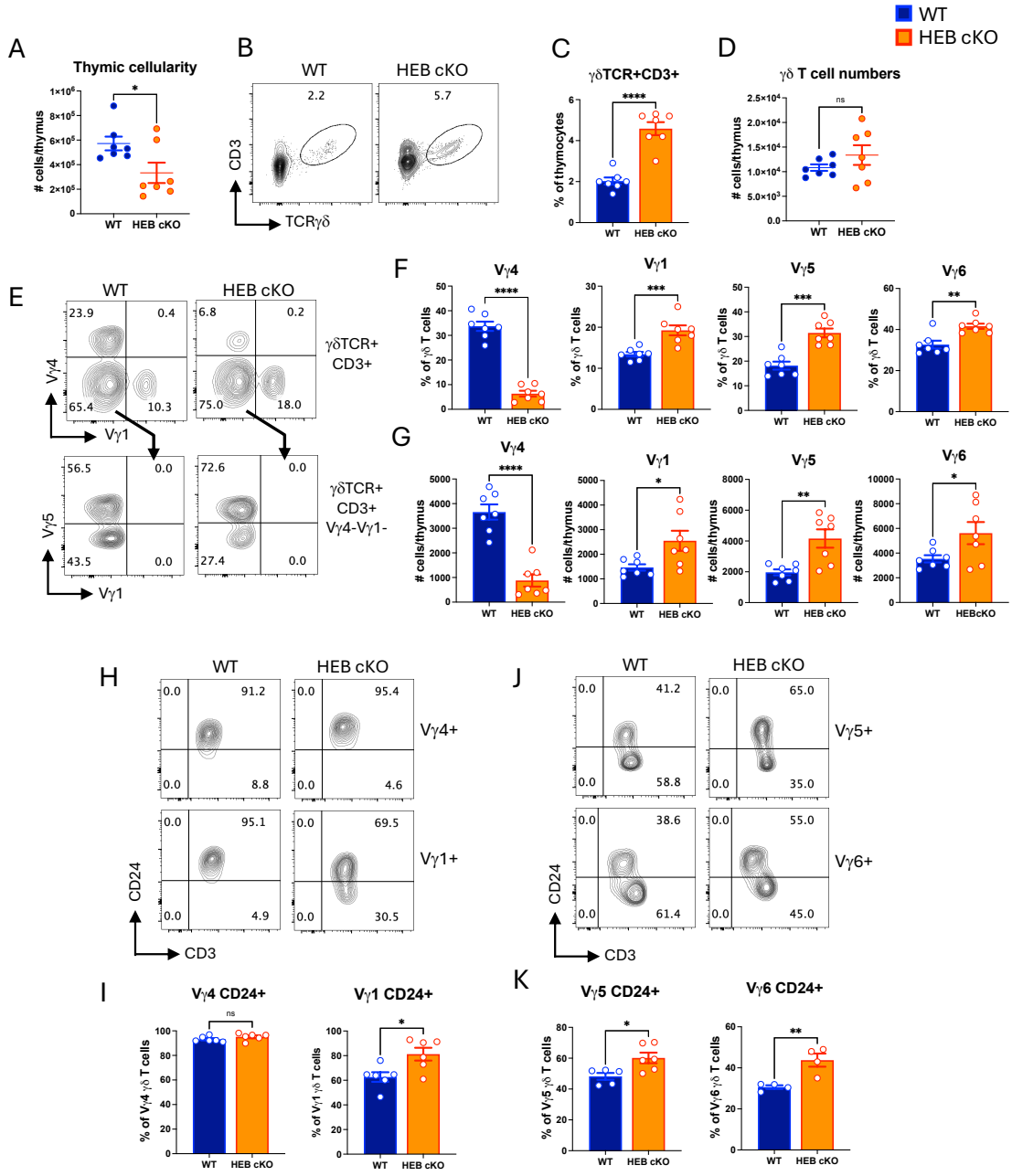


**Figure 1. Decreased Vγ4$^{+}$ γδ T cells and increased immature γδ T cells in E18 fetal thymocytes from HEB cKO mice compared to WT.** WT and HEB cKO mice were set up for timed matings to produce WT and HEB cKO littermates. E18 thymocytes analyzed by flow cytometry. **A**. Numbers of cells per thymus. **B, C**. Representative flow plots (**B**) and percentages

(**C**) of γδ T cells. **D**. Absolute numbers of γδ T cells per thymus. **E, F**. Representative contour plots (**E**) and percentages (**F**) of Vγ4 and Vγ1 cells out of all γδ T cells. **G**. Absolute numbers of Vγ subset cells per thymus. **H, I**. Representative contour plots (H) and percentages (I) of $CD24^+$ cells within Vγ4 and Vγ1 subsets. **J.** Representative contour plot of Vγ5 and Vγ6 CD24 expression in the $V\gamma4^-V\gamma1^-$ population. **K**. Percentages of $CD24^+$ cells in Vγ5 and Vγ6 subsets out of all γδ T cells. Blue = WT, orange = HEB cKO. Data is presented as mean +/- SEM. Statistical significance was assessed using unpaired student's T tests. ****p <0.0001, ***p < 0.005, **p < 0.001, *p < 0.05, n=non-significant.

---

**Shifts in γδ T cell subset populations in E18 HEB cKO γδ T cells**

To understand the molecular basis of these differences, we conducted single cell RNA sequencing (scRNA-seq) on $\gamma\delta TCR^+CD3^+$ T cells sorted from E18 WT and HEB cKO fetal thymuses. After quality control, the datasets were merged, myeloid cells were excluded, and cell cycle genes were regressed (see Methods and R-markdown files for details). The resulting merged dataset was subjected to principal component analysis (PCA) to generate uniform manifold alignment plots (UMAPs) (**Fig. 2A-C**). Eight clusters (numbered 0-7) were identified (**Fig. 2A**), some of which had different proportions of WT versus HEB cKO cells (**Fig. 2B, C**). Of note, a split UMAP (**Fig. 2C**) showed that HEB cKO cells were entirely missing in cluster 4 (green), and poorly represented in cluster 2 (red). By contrast, the cells in cluster 3 (pink) were nearly all HEB cKO cells, and clusters 1 (light gray) and 0 (dark gray) were highly enriched in HEB cKO cells. Clusters 5 (blue), 6 (orange) and 7 (maroon) had strong representation of both WT and HEB cKO cells. To assign identities to these clusters, we generated a heatmap of the 10 most differentially expressed genes in each cluster relative to all other clusters (**Fig. 2D**) and assessed the relative expression of curated

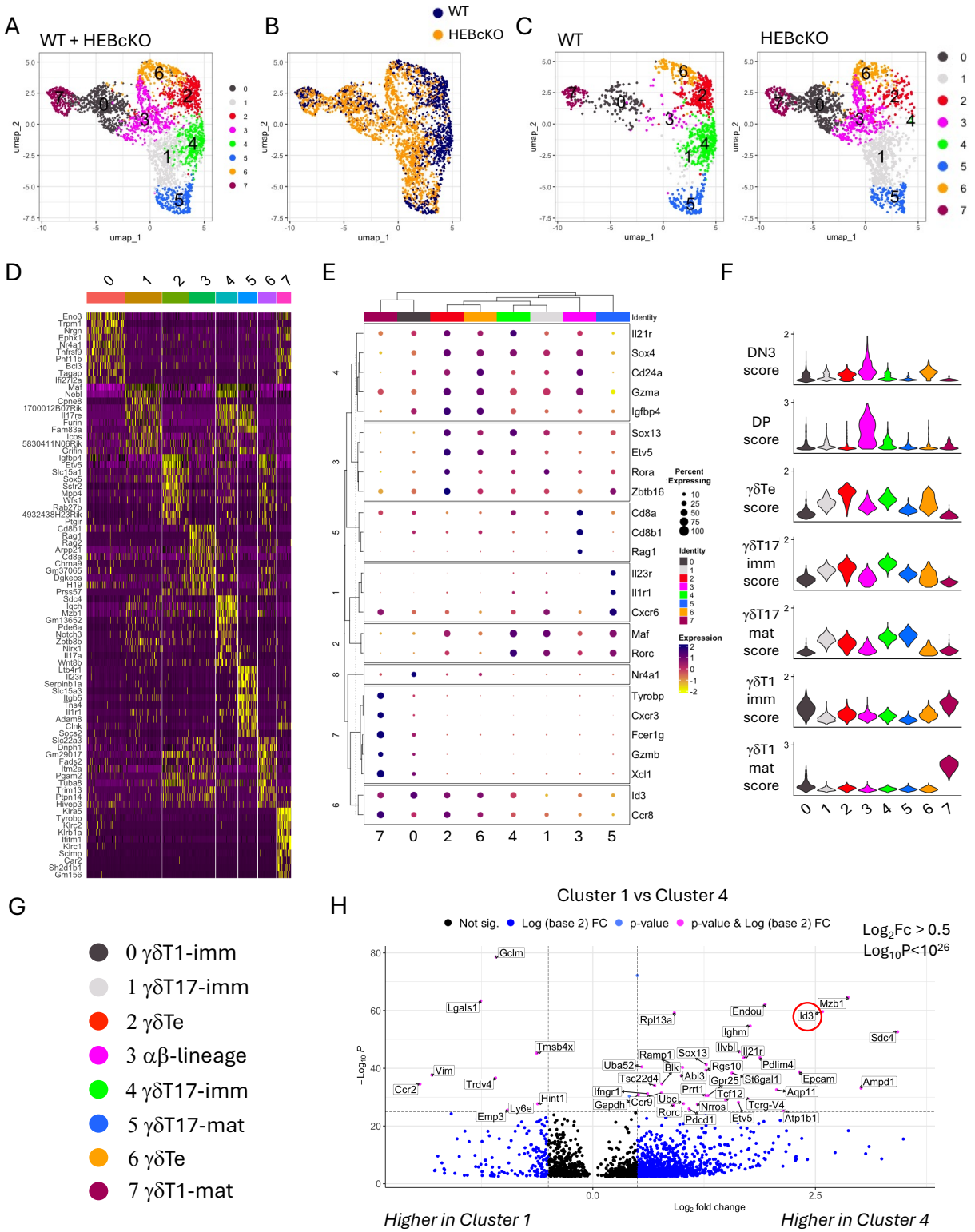


**Figure 2. Single cell RNA-sequencing of E18 γδTCR$^+$ fetal thymocytes reveals perturbations in Vγ and Vδ expression and early γδ T cell regulators in HEB cKO fetal thymus.** E18

γδTCR$^+$CD3$^+$ thymocytes were sorted from WT and HEB cKO littermates, subjected to scRNA-seq, and analyzed using R-Seurat. **A**. UMAP plot of merged data from WT and HEB cKO cells revealing 8 clusters (0-7). **B**. UMAP plot grouped by WT (blue) and HEB cKO (orange) cells. **C**. Split UMAP plot showing location and proportions of WT cells (left) and HEB cKO cells (right) within the UMAP. **D.** Single cell heatmap depicting the 10 most differentially expressed genes between all clusters. **E**. Clustered dot plot showing the proportions and levels of curated genes in each cluster. **F**. Violin plots of the relative magnitude of gene set modules in each cluster. **G**. Identities assigned to each cluster based on the analysis in (A-F). **H**. Enhanced volcano plot depicting differentially expressed genes between cluster 4 and cluster 1. Pink dots = statistically significant $Log_2Fc$ and $Log_{10}P$. Red circle highlights that Id3 is severely decreased in Cluster 1 relative to Cluster 4.

---

γδ and αβ T cell genes between different clusters with a clustered dot plot (**Fig. 2E**). This analysis showed the degree of similarity between clusters, using scores derived from individual genes. We also generated gene lists diagnostic for DN3 cells, DP cells, early γδ T, immature γδT1 cells (γδT1 imm), and mature γδT1 cells (γδT1 mat), based on previous studies (*65, 66*), and used them to create module scores for each cluster (**Fig. 2F**). Only cells co-expressing all genes within a module gene list ("AND" gated in Boolean logic) were included in each module. Applying these criteria allowed us to assign identities to each cluster (**Fig. 2G**).

Interestingly, both Cluster 1 (gray) and Cluster 4 (green) fell into the γδT17-imm bin (**Fig. 2F, G**) and were more closely related to each other than to any of the other clusters (**Fig. 2E**). Since Clusters 4 and 1 were largely confined to WT or HEB cKO, respectively, we set out to identify

genes differentially expressed between them in an unbiased manner by generating an enhanced volcano plot (**Fig. 2H**). Remarkably, many of the most differentially expressed genes were immediately recognizable as signature genes of γδ T cell precursors, including *Ccr9*, *Rorc*, *Ifngr1*, *Etv5*, *Il21r*, *Blk*, and *St6gal1* (*66*). These genes were highly expressed in WT cells (Cluster 4) but not in HEB cKO cells (Cluster 1), suggesting that HEB is required for the establishment of the early γδ T cell gene network. We also noted decreased levels of *Id3* in Cluster 1(red circle). Since *Id3* upregulation can be a consequence of TCR signaling, this finding suggested a disruption of γδTCR signaling, a role for HEB in *Id3* expression, or both.

**Diversion to αβ fate and paucity of early γδ T cell precursors among HEB cKO cells**

We next examined the relative module scores of WT cells versus HEB cKO cells (**Fig. 3**). The developmental subset modules shown in Fig. 2 were supplemented with three additional modules that identified cells co-expressing the genes encoding obligate fetal TCRγ-TCRδ receptor pairs: 1) Vγ5 and Vδ1 (*Tcrg-V5, Trdv4*), 2) Vγ6 and Vδ1 (*Tcrg-V6, Trdv4*), and 3) Vγ4 and Vδ5 (*Tcrg-V4, Trdv5*). We did not detect genes encoding Vγ7 (*Tcrg-V7*) or Vδ6.3 (*Trav15d-1-dv6d-1)*, consistent with previous reports (*23*) and supporting our designation of $V\gamma4^{-}5^{-}1^{-}$ cells as Vγ6 cells. Comparisons of module score distributions in WT versus HEB cKO cells by split UMAPs revealed striking differences. Relative to WT, HEB cKO cells in the αβ population (cluster 3) had a mildly elevated DN3 signature (**Fig. 3A**), and a greatly increased DP signature (**Fig. 3B**). Most WT cells in clusters identified as γδTe (clusters 2, 6) and γδT17 imm (cluster 4) co-expressed Vγ4 and Vδ5 (**Fig. 3C**) and displayed strong γδTe (**Fig. 3D**) and immature γδT17 (**Fig. 3E**) scores. By contrast, very few HEB cKO cells exhibited Vγ4 Vδ5 co-expression. Furthermore, the γδTe score was weak and the immature γδT17 signature was nearly absent in

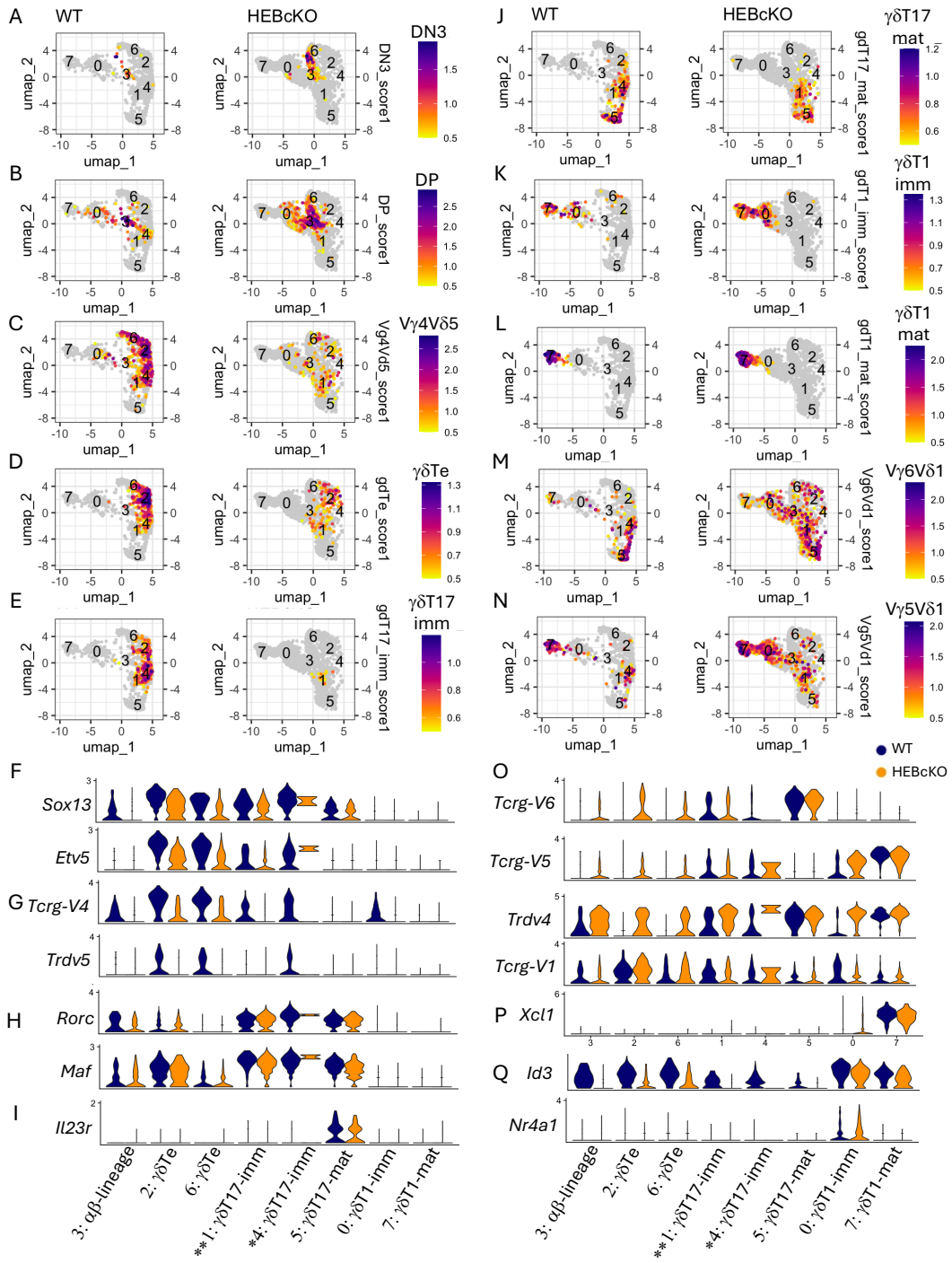


**Figure 3**. **Disruptions of Vγ and Vδ element expression and early γδ T cell precursor gene expression in fetal HEB cKO γδ T cells.** Gene sets diagnostic for cells belonging to specific developmental subsets and cells with Vγ-Vδ paired expression were assembled and used to

generate module scores. Module scores were applied to split UMAP plots, allowing a detailed comparison between WT and HEB cKO cells (A-E, J-N). Split violin plots (blue=WT, orange=HEB cKO) were generated for specific genes belonging to these modules (F-G, O-Q), revealing differences in expression within each cluster. The cluster numbers and names depicted below the violin plots correspond to the numbers on the UMAPs and the identities assigned to those clusters in Fig. 2G. Clusters composed mostly of WT cells (*4) or HEBcKO cells (**1) are designated by asterisks.

---

HEB cKO cells. We also examined differential expression of specific genes between WT and HEB cKO cells within each cluster using split violin plots (**Fig. 3F-I**) and split feature plots (**Fig. S2**) of single genes. Expression of the γδTe regulators *Sox13* and *Etv5* was lower in HEB cKO cells than in WT cells (**Fig. 3F**, **Fig. S2**). Moreover, HEB cKO cells displayed severely diminished expression of *Tcrg-V4* and *Trdv5* was undetectable (**Fig. 3G, Fig. S2**). By contrast, the second stage regulators *Rorc* and *Maf* did not exhibit major differences in expression between HEB cKO and WT cells (**Fig. 3H, Fig. S2**). Since *Rorc* and *Maf* are expressed throughout γδT17 development, albeit at different levels, we also examined expression of *Il23r*, which is restricted to the mature γδ T subset within the γδ cell lineage but observed no differences between WT and HEB cKO cells (**Fig. 3I**).Together, these results suggest that HEB cKO cells that survive the immature stages of γδT17 development do not require HEB to upregulate key regulators of the mature γδT17 gene program.

**Increased proportions of immature Vγ6 Vδ1 and Vγ5 Vδ1 cells in HEB cKO mice**

We also compared the distribution of γδT17 and γδT1 module scoring in WT versus HEB cKO cells using split feature plots (**Fig. 3J-L**). In both WT and HEB cKO cells, the mature γδT17 module was concentrated in clusters 1, 4, and 5 (**Fig. 3J**), the immature γδT1 score was limited to clusters 0 and 7 (**Fig. 3K**), and the mature γδT1 score was restricted to cluster 7 (**Fig. 3L**), suggesting little to no perturbation in γδT1 development. In WT cells, the Vγ6 Vδ1 co-expression score was primarily found in clusters scoring high for the mature γδT17 module (**Fig. 3M**), and Vγ5 Vδ1 co-expressing cells were mainly associated with cluster 7 (**Fig. 3N**). By contrast, Vγ6 Vδ1 co-expressing cells from HEB cKO mice were abundant in many different clusters, including those that scored highly for γδTe module (clusters 2 and 6). HEB cKO Vγ5 Vδ1 cells were likewise more widely distributed, with strong representation in cluster 0, consistent with an immature γδT1 cell identity. These observations are consistent with an increase in immature Vγ6 and Vγ5 cells in the HEB cKO fetal thymus, as suggested by flow cytometry (**Fig. 1**).

The underlying basis of these differences were further probed with split violin plots of the expression of individual genes in WT versus HEBcKO cells within each cluster (**Fig. 3O-Q**). WT cells expressing *Tcrg-V6*, *Tcrg-V5*, or *Trdv4* were restricted to the clusters that also co-expressed Vγ6-Vδ1 (clusters 4, 5) or Vγ5-Vδ1 (cluster 7), whereas expression of each of these genes in HEB cKO cells occurred both within and outside those clusters (**Fig. 3O**). *Tcrg-V1*, which does not have a canonical pairing partner during fetal γδ T cell development, was expressed across all clusters at the transcriptional level in both WT and HEB cKO cells. We verified that the mature γδT1 program was restricted to cluster 7 in both WT and HEB cKO cells by examining expression of *Xcl1* (**Fig. 3P**).

**Failure of *Id3* upregulation in γδTe and immature γδT17 cells but not γδT1 cells**

Given the difference in *Id3* expression in Clusters 1 and 4, we assessed *Id3* expression in WT versus HEB cKO cells in split violin plots (**Fig. 3Q, Fig. S2**). In WT cells, *Id3* was upregulated in αβ (DN3/DP; cluster 3) and γδTe (clusters 2, 6) cells, consistent with the timing of γδTCR signaling at the αβ/γδ T cell checkpoint, and to a lesser extent in immature γδT17 cells (cluster 4). *Id3* was also high in immature γδT1 (cluster 0) and mature γδT1 cells (cluster 7). In contrast, *Id3* expression was undetectable in HEB cKO cells in αβ (cluster 3) and γδT17 imm (cluster 1), and decreased in γδTe cells (clusters 2, 6) relative to WT. These results indicate that HEB deficiency severely blunts *Id3* upregulation in cells expressing the Vγ and Vδ chains associated with the γδT17 fate. However, *Id3* expression levels were equivalent between WT and HEB cKO cells in immature and mature γδT1 cells (clusters 0 and 7). Furthermore, *Nr4a1* was upregulated in immature γδT1 cells (cluster 0) in both WT and HEB cKO cells (**Fig. 3Q**), consistent with intact cellular perception of strong TCR signaling (*67*). Therefore, HEB is required for *Id3* upregulation during γδT17 development but not during γδT1 development.

**Unperturbed αβ T cell development in the E18 fetal thymus of Id3-KO mice**

To assess whether the decrease in *Id3* expression has an impact on γδ T cell development, we examined E18 thymocytes from Id3-KO mice. Previous studies of γδ T cell development in adult Id3-KO mice were hampered by a major expansion of mature $V\gamma1.1^{+}V\delta6.3^{+}$ cells and IL-4 dependent induction of innate CD8 T cell development (*68, 69*). This expansion does not occur until after birth (*70*), allowing us to examine the impact of *Id3*-deficiency on fetal γδ T cell development without this confounding factor. Since the phenotype of *Id3* deficiency in the thymus can be muted in certain strains of mice (*71*), we first examined the phenotype of thymocytes in

adult Id3-KO mice. Id3-KO mice had a marked decrease in thymic cellularity relative to WT (**Fig. S3A**). Id3-KO thymocytes also exhibited an increase in DN and CD8 SP thymocytes, and a decrease in DP cells, while the percentages of CD4 T cells were similar (**Fig. S3B, C**), and these patterns were recapitulated for the most part by absolute cell numbers (**Fig. S3D**). Furthermore,

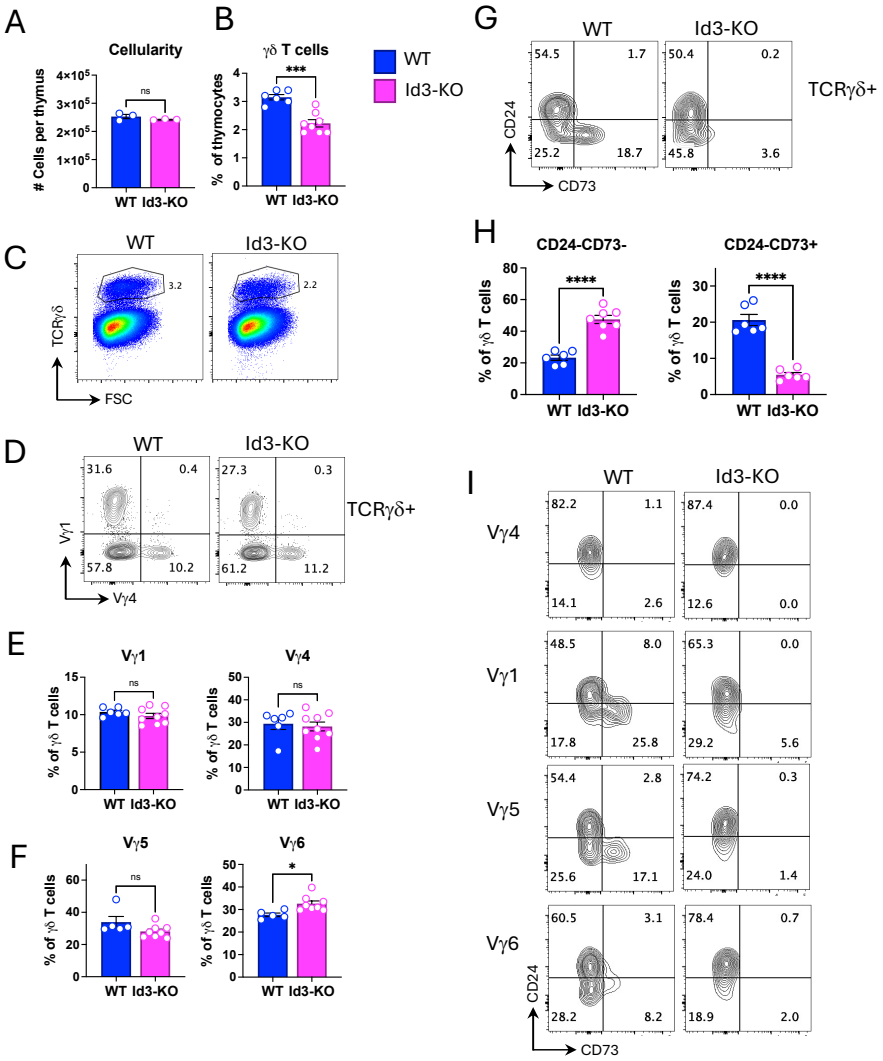


**Figure 4. Fetal thymus of Id3-deficient mice fail to upregulate CD73 during γδ T cell development.** E18 thymocytes were obtained from WT and Id3-KO mice and analyzed by flow cytometry. **A.** Absolute numbers of cells per thymus. **B, C**. Percentages (B) and representative

flow cytometry plots (C) of γδ T cells in E18 fetal thymus. **D, E**. Representative flow plots (D) and percentages (E) of Vγ1$^+$ and Vγ4$^+$ γδ T cells out of all γδ T cells. **F**. Percentages of Vγ5 and Vγ6 cells out of all γδ T cells. **G**. Representative flow plots showing CD24/CD73 subsets within the γδ T cell population. **H.** Percentages of mature (CD24$^-$) CD73$^-$ and CD73$^+$ cells out of all γδ T cells. **I**. Representative flow plots depicting CD24/CD73 subsets within each Vγ subset. Plots are gated on Vγ chains as indicated. Blue = WT, pink = Id3-KO. Data is presented as mean +/- SEM. Statistical significance was assessed using unpaired student's T tests. ****p <0.0001, *p < 0.05, n=non-significant.

---

we observed a large increase in thymic γδ T cells in the Id3-KO thymus (**Fig. S3E, F**), nearly all of which were Vγ1.1$^+$Vδ6.3$^+$CD24$^-$CD73$^+$ γδ T cells (**Fig. S3H, I**). By contrast, E18 fetal thymocytes from Id3-KO mice had equivalent percentages of DN and DP cells (**Fig. S4**) and normal cellularity (**Fig. 4A**). The proportions of γδ T cells were slightly decreased relative to WT mice (**Fig. 4B, C**). Therefore, E18 fetal thymocytes from Id3-KO mice did not exhibit any of the characteristics related to Vγ1 Vδ6.3 cell expansion seen in the adult, permitting an analysis of the impact of *Id3* deficiency on γδT1/γδT17 lineage choice.

**Defects in CD73 upregulation and IL-17 production in fetal γδ T cells from Id3-KO mice** We next examined γδ T cell subsets in E18 Id3-KO fetal thymus. Vγ chain usage in γδ T cells in fetal Id3-KO thymus was very similar to WT, with a small increase in the proportion of Vγ6 cells (**Fig. 4D-F**). However, there was a striking loss of CD73$^{+}$ cells among Id3-KO γδ T cells, accompanied by a corresponding increase in the percentages of CD73$^{-}$ cells (**Fig. 4G, H**). Vγ subset specific

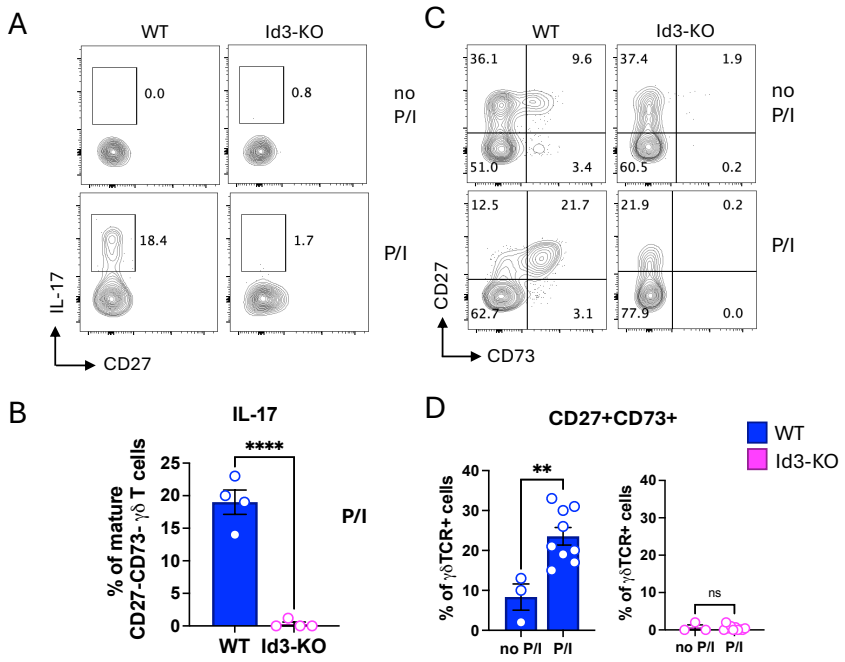


**Figure 5. Id3-KO γδ T cells fail to produce IL-17 in response to stimulation.** Fetal thymocytes were harvested at E18 and cultured with or without PMA/ionomycin (P/I) for four hours in the presence of brefeldin A, followed by flow cytometry. **A**. Representative flow cytometry plots showing IL-17 expression in the γδTCR$^{+}$CD3$^{+}$Vγ5$^{-}$Vγ1$^{-}$CD24$^{-}$CD27$^{-}$CD73$^{-}$ population (primarily mature Vγ6 cells) at baseline (top) or after stimulation (bottom), as assessed by intracellular staining. **B**. Percentages of stimulated cells expressing IL-17; note that IL-17 was not expressed outside this population. **C**. Representative flow plots showing CD73 expression at baseline (top) and after stimulation by P/I (bottom) within the γδ T cell population. **D.** Quantification of

percentages of $CD27^+CD73^-$ cells and $CD27^+CD73^+$ cells at baseline (top) or after stimulation (bottom) within the WT (left) or Id3-KO (right) populations. Blue bars =WT, Pink bars = Id3-KO. Statistical significance was determined using Student's t-tests, ****p <0.0001, ***p < 0.005, **p < 0.001, n=non-significant.

---

analysis confirmed that CD73 expression was lost in both Vγ5 and Vγ1 cells (**Fig. 4I**), suggesting that these cells might perceive a weaker γδTCR signal and be diverted into the γδT17 lineage. To assess this possibility, we stimulated *ex vivo* E18 fetal thymocytes from WT and Id3-KO mice with PMA/ionomycin and examined IL-17 production by intracellular flow cytometry. WT γδ T cells produced IL-17, but Id3-KO γδ T cells did not (**Fig. 5A, B**).

Given this observation, we considered the possibility that the absence of *Id3* could derail the TCR signaling outcomes needed for IL-17 programming. Since CD73 can be upregulated in response to strong γδTCR signaling (*49*), we measured CD73 surface expression on WT and Id3-KO γδ T cells with and without 4 hrs of PMA/ionomycin (P/I) treatment. Prior to stimulation, $CD27^+CD73^-$ and $CD27^+CD73^+$ cells were present in the WT population, whereas $CD27^-$ and $CD27^+$ cells from Id3-KO mice were both CD73 negative. Stimulation resulted in an increase in the proportion of WT $CD27^+CD73^+$ γδ T cells, whereas Id3-KO cells remained CD73 negative (**Fig. 5C, D**). These results indicate that the impact of *Id3* loss occurs downstream of the PI3K and NFAT signaling pathways mimicked by P/I treatment. Of note, PI3K is an important mediator of γδTCR signaling in γδT17 development (*46*).

**Impaired maturation of γδT17 cells in Id3-KO fetal thymocytes**

We next examined expression of the second stage γδT17 regulators MAF, PLZF, and RORγt in WT and Id3-KO E18 γδ T cells by intracellular low cytometry. In WT Vγ4 cells, which are primarily immature, about 25% of the cells co-expressed MAF and PLZF at intermediate levels, consistent with priming towards the γδT17 lineage (**Fig. 6A, B**). However, this population was significantly dampened in

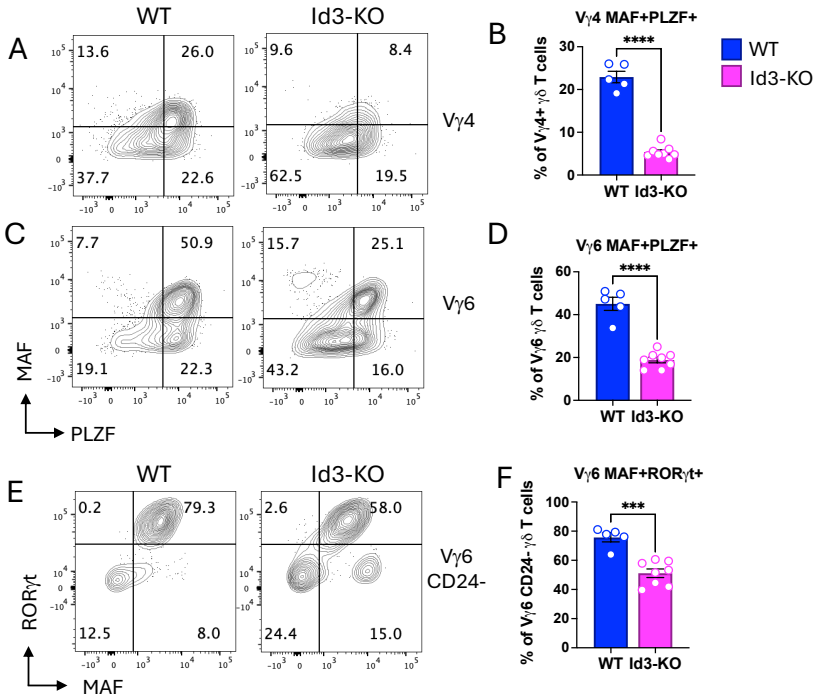


**Figure 6. Immature γδ T cells in Id3-KO E18 thymus exhibit decreased expression of MAF and PLZF**. E18.5 fetal thymocytes were harvested from WT and Id3-KO mice and subjected to intracellular flow cytometry. Cells were gated on γδTCR$^{+}$CD3$^{+}$ Vγ1$^{-}$Vγ5$^{-}$γδTCR$^{+}$CD3$^{+}$ cells to enrich for γδ T cells with γδT17 potential. **A, B.** Representative flow plots of MAF and PLZF expression in Vγ4$^{+}$TCRγδ$^{+}$CD3$^{+}$ cells from WT versus Id3-KO mice. **B**. Percentages of Vγ4$^{+}$ cells co-expressing MAF and PLZF. **C.** Representative flow plots showing MAF and PLZF expression

in Vγ6 cells. **D**. Percentages of Vγ6 cells co-expressing MAF and PLZF. **E**. Representative flow plots showing RORγt and MAF expression in mature CD24$^-$ Vγ6 cells. **F**. Percentages of mature CD24$^-$ Vγ6$^+$ γδ T cells co-expressing RORγt and MAF. Blue bars =WT, pink bars = Id3-KO. Statistical significance was determined using Student's t-tests, ****p <0.0001, ***p < 0.005.

---

Id3-KO mice. Vγ6 cells from Id3-KO mice also exhibited a decrease in the proportion of mature γδT17 cells relative to WT (**Fig. 6C, D**). To further assess the impact of *Id3* deficiency on mature Vγ6 transcription factor expression, we gated on CD24$^-$ cells within the Vγ6 populations (**Fig. 6E, F**). The majority of cells from WT mice co-expressed RORγt and MAF, consistent with programming into the γδT17 lineage. However, the RORγt$^+$MAF$^+$ population was decreased in mature Id3-KO Vγ6 cells indicating impaired γδT17 differentiation in the absence of *Id3*. Our results thus indicate that *Id3* is an important driver of γδT17 cell maturation.

**Intact early γδ T cell regulatory program in the Id3-KO fetal thymus**

To more globally assess changes in Id3-KO γδ T cell populations, we performed scRNA-seq on DN cells magnetically enriched from E18 WT and Id3-KO fetal thymuses. After quality control, the datasets were merged, and the resulting merged dataset was subjected to PCA to generate UMAP plots. Eleven clusters were defined (0-10) (**Fig. 7A**), with representation from both WT and Id3-KO cells in most clusters (**Fig. 7B**). Many of the clusters were identified as DN3 or DN4 subsets, based on expression of *Il2ra* and *Ptcra* (**Fig. 7C, D**). However, two small clusters were identified as γδ T lineage cells based on co-expression of *Sox13*, *Etv5*, *Maf*, and *Zbtb16* (cluster 6)

or co-expression of *Xcl1* and *Zbtb16* (cluster 9). Clusters 6 and 9 were subsetted and re-clustered,

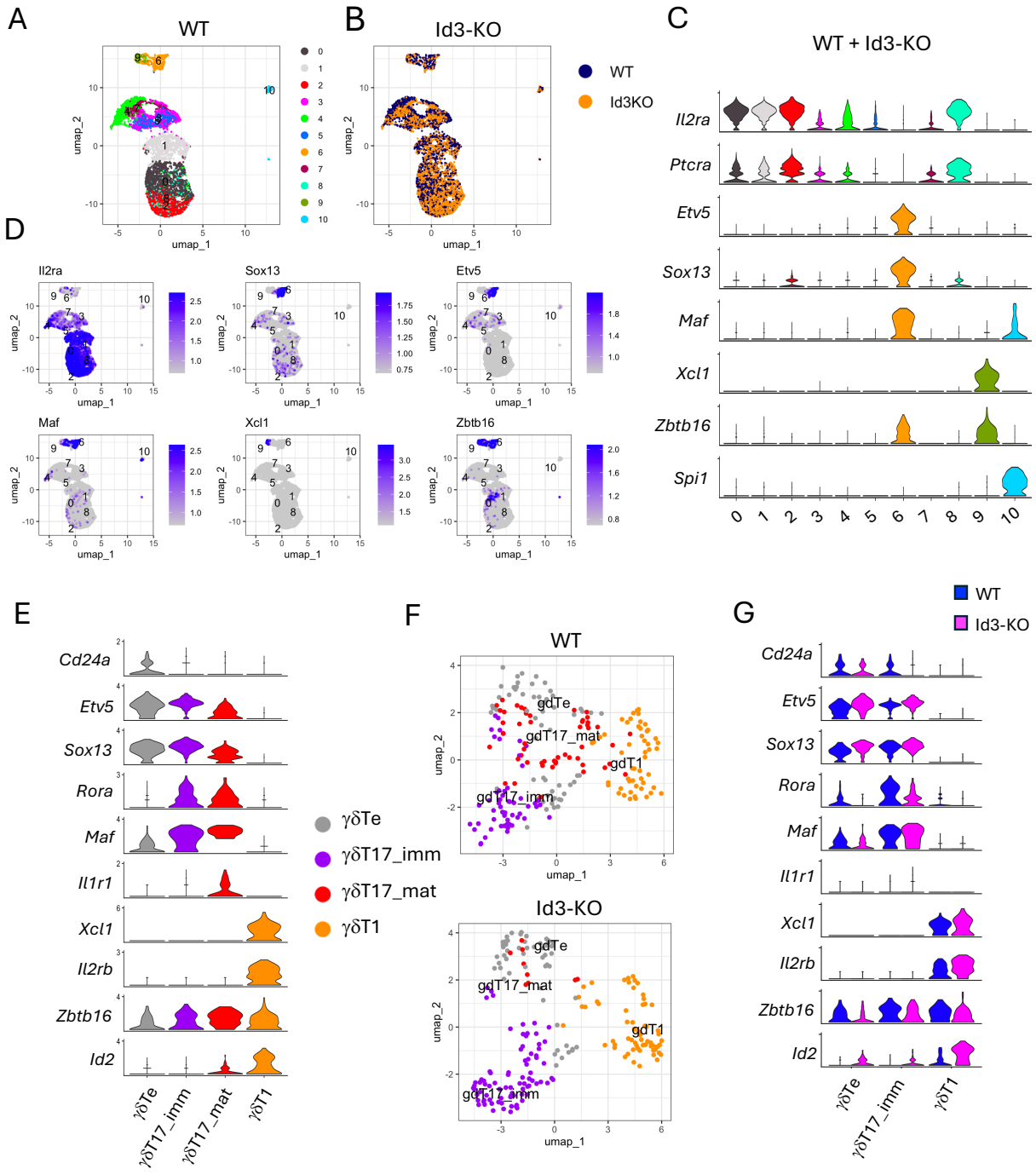


**Figure 7. Diminished expression of second stage but not first stage regulators in Id3-KO E18 γδ T cells as assessed by scRNA-seq.** E18 thymocytes from WT and Id3-KO mice were harvested

and enriched for DN (double negative; $CD4^-CD8^-$) cells by magnetic sorting. Sorted cells were subjected to scRNA-seq. **A**. UMAP plot of the merged dataset showing clustering. **B**. Grouped UMAP plot of merged dataset showing WT versus Id3-KO cells. **C**. Violin plots showing relative expression of specific genes within each cluster. **D**. Feature maps showing expression of different genes in merged dataset. Clusters (6, 9) containing γδ T cells were re-clustered for analysis, generating four new clusters that were classified into early γδ T cell precursors (gdTe, gray), immature γδT17 cells (gdT17_imm, purple), mature γδT17 cells (gdT17_mat, red), and γδT1 cells (gdT1, orange). **E**. Violin plots of gene expression used to assign lineages and developmental stages to the clusters. **F.** Split UMAP plots depicting WT cells (top) and Id3-KO cells (bottom) in the merged γδ T cell dataset. **G**. Split violin plots showing relative expression of these genes in WT (blue) versus Id3-KO (pink) knockout cells within the gdTe, gdT17_imm, and gdT1 clusters. The gdT17_mat cluster was excluded from this analysis due to the paucity of Id3-KO data points.

---

resulting in four new clusters which were classified using violin plots of diagnostic genes into γδTe (gray), γδT17 imm (purple), γδT17 mat (red), and γδT1 (orange) subsets (**Fig.7E**). Notably, a split UMAP plot showed that the γδT17 mat population was less robust among Id3-KO cells than in WT cells (**Fig. 7F**). This cluster was excluded from further analysis. Next, we generated split violin plots to examine the expression of individual genes in WT versus Id3-KO cells (**Fig. 7G**). Levels of *Etv5* and *Sox13* were not diminished in γδTe and γδT17 imm cells from Id3-KO mice, indicating that γδ T cell commitment was relatively unaffected by the absence of *Id3*. However, *Rora*, *Maf*, and *Zbtb16* mRNA levels were lower in Id3-KO cells, most markedly in γδTe and γδT17 cells, whereas γδT1 gene expression (*Xcl1*, *Il2rb*, *Id2*) was unperturbed. These finding suggested that in spite of their failure to express CD73, γδT1 cells can develop independently of Id3. Notably, *Id2*

was ectopically induced at low levels in Id3-KO cells in γδTe and γδT17 cells and was elevated in γδT1 cells (**Fig. 7G**), suggesting it may have provided partial compensation for the loss of *Id3* in the fetal thymus, as it is believed to do in the adult thymus (*71*).

## DISCUSSION

γδ T cell development occurs via a two-step process, in which γδ-lineage commitment is followed by functional maturation (*65, 72*), but how these two events are orchestrated is not well understood. Here we show that HEB and Id3 participate in a negative feedback loop that allows HEB-dependent γδ T cell specification to be followed by Id3-dependent γδ T cell maturation. These findings are consistent with the TCR signal strength model but reveal additional levels of complexity. First, HEB is instrumental in shaping the TCRγ and TCRδ repertoire at the level of V element gene expression. Secondly, HEB is required for *Id3* expression downstream of TCR signaling in Vγ6 Vδ1 γδ T cells but not Vγ5 Vδ1 γδ T cells, which develop independently of HEB. In addition, HEB and Id3 regulate distinct stages of γδT17 cell development, with a requirement for HEB for expression of first stage regulators, and Id3 important in the elaboration of second stage regulators. Thus, absence of either HEB or Id3 resulted in a failure of functional programming to the γδT17 fate. Together, these studies have uncovered an HEB-dependent switch that enables the transition from committed γδ T cell precursors to mature γδT17 effector cells.

Our work reveals that HEB shapes the fetal γδTCR repertoire to a much greater degree than previously appreciated. Most studies on E protein regulation of *Tcrg-V* and *Trdv* elements have been focused on E2A (*38*). E2A can bind directly to the *Tcrg-V4* promoter, and is needed for Vγ4 expression in the adult thymus (*73, 74*). By contrast, we found that Vγ4$^+$ cells are present in the adult thymus (*27*), but scarce in the fetal thymus, where expression of *Tcrg-V4* and *Trdv5* are compromised at the transcriptional level. Loss of E2A lifts repression of *Tcrg-V5* and *Trdv4*, resulting in an aberrant population of Vγ5$^+$ γδ T cells in the thymus (*73*). We did not observe Vγ5$^+$ cells in the adult thymus of HEB cKO mice. However, we found a strong de-repression of *Trdv4*

in fetal γδ T cell populations, consistent with E protein-dependent silencing elements in the *Trdv4* locus that restrict *Trdv4* expression in the adult thymus. Together, these findings suggest that HEB and E2A collaborate to restrict temporal *Trdv4* expression. Intriguingly, E proteins directly control the expression of *Trav15d-1-dv6d-1* (which encodes Vδ6.3) as well, which dictates the γδT1 fate choice by strong induction of *Id3* in Vγ1.1 Vδ6.3 cells (*75*). Thus, the E protein/Id3 axis is instructive upstream of TCR signaling in multiple γδ T cell subsets.

Our studies also support important roles for HEB and Id3 in coupling γδTCR signal strength to γδ T cell fate choices. T cell precursors lacking HEB were impaired in their ability to coordinately express genes involved in γδ T cell commitment and install the early γδ T cell gene network. In addition, HEB or Id3 deficiency each appeared to alter the cellular perception of TCR signal strength, in opposite ways, as measured by an increase or decrease, respectively, in CD73 expression (*27, 49*). However, mature Vγ5$^+$ cells emerged with intact signature genes in both cases, and Id3 was upregulated in Vγ5$^+$ cells independently of HEB. Therefore, it is possible that HEB collaborates with Egr factors to induce *Id3* under conditions of intermediate TCR signal strength, whereas high levels of Egr may be sufficient for *Id3* upregulation under conditions of strong γδTCR signaling.

Maturation of most γδ T cell precursors into γδT17 cells requires TCR signaling, but other signaling pathways, such as SLAM family members, cytokine receptors, Notch receptors, and co-stimulatory molecules are also essential for γδ T cell functional lineage choice (*41, 48, 76-78*). We have previously shown that cytokine receptor signaling can decrease *Id3* mRNA levels during strong γδTCR signaling (*48*), suggesting that an intersection between signaling pathways may keep Id3 levels high enough to suppress αβ T cell gene expression but low enough to allow γδT17 gene

expression. This may help to explain the ability of Vγ6 cells to develop into γδT17 cells in the presence of strong TCR signaling (*40*). HEB has also been linked to several signaling pathways that can regulate activity or gene target specificity. A short form of HEB, HEBAlt can be activated by a JAK-dependent pathway, suggesting a possible connection to cytokine receptors such as IL-7, IL-21 and IL-23 (*79*). The N-terminus of the long form of HEB, HEBCan, can complex with members of the ETO co-repressor family to directly inhibit gene expression. HEB factors can also collaborate directly with SMAD transcription factors, which are activated downstream of TGFβ, in embryonic stem cells (*80*). The context-dependence of these interactions suggest that HEB and/or E2A may regulate distinct sets of genes as progenitor cells migrate through the thymus.

There are several caveats to this study. Our *ex vivo* examination of E18 γδ T cells by flow cytometry and scRNA-seq provided a snapshot of developing γδ T cells with high relevance to γδT17 cells but leaves open the possibility HEB could play roles in γδ T cell development at different time points that were not captured in our analysis. In addition, it is currently unclear whether the diminished expression of second stage regulators such as PLZF and MAF is a cause or a consequence of impaired maturation of γδ T cell precursors. It also remains to be determined whether the first stage regulators are direct targets of HEB factors, and what the relative roles of HEBAlt and HEBCan might be in these processes. We have also not addressed the relationship between E18 γδT17 cells with a subset of γδT17 cells that arise from fetal precursors independently of TCR signaling (*51*), although *Id3* could be induced by a combination of HEB and non-TCR signaling pathway(s), which might result in similar dynamics. Additional studies will be needed to address these questions.

Our studies have revealed multiple negative feedback loops between E proteins and Id factors that occur during T cell development. In developing γδ T cells, HEB upregulates *Id3* expression. Id3 in turn suppresses E protein activity. When *Id3* fails to be upregulated in Id3-KO γδ T cell precursors, HEB activity is uninterrupted, leading to the activation of Id2 expression. As waning E protein activity leads to the cessation of *Id3* transcription, the HEB-Id3 interactions comprise a self-limiting feedback loop. Our results also show that Id2 and Id3 are not equivalent, since Id2 can at least partially compensate for Id3 in β-selection and γδ-selection in the fetal thymus but is insufficient for γδT17 maturation. Together, our studies have identified a role for HEB in inducing the early γδ T cell gene regulator network while also launching the γδT17 maturation network by activating *Id3* expression. Further studies identifying direct targets and partners of HEB in early γδ T cell precursors and mature γδT17 cells will be necessary to fully understand the impact of shifting ratios of HEB, Id3, and Id2 on γδ T cell development.

## MATERIALS AND METHODS

### Experimental Design and Statistical Analysis

The overall goal of this study was to better understand how HEB transcription factors regulate the transcriptional networks required for the development of IL-17 producing γδ T cells. The subjects of these studies were genetically modified mice. The experimental variable was the genotype of the mice, chosen based on availability of experimental animals and littermate controls. For the scRNA-seq experiments, fetal thymocytes of like genotype from 3 or more mice were pooled prior to enrichment. Each flow cytometry analysis was performed using 3 or more mice of like genotype per experiment, repeated 2-3 times. Mice of both sexes were used, and since no sex differences were apparent, data were pooled. Each datapoint depicted in graphs represents an individual mouse, providing biological replicates. The investigators were not blinded to allocation during experiments and outcome assessment, except when fetal thymocytes were individually analyzed by flow cytometry prior to genotyping. Significance of pairwise data was computed by unpaired two-tailed Student's t-test, with $p < 0.05$ considered statistically significance. The error bars represent standard error of the mean (SEM) values.

### Mice

$HEB^{fl/fl}$ mice have loxP sites flanking exons that encode the bHLH DNA binding and dimerization domain (*63*). These mice were bred to Vav-iCre transgenic mice (JAX stock #008610) (*81*), which deletes in all hematopoietic cells (*82*), to generate $HEB^{fl/fl;Vav\text{-}iCre}$ (HEB cKO) mice, as previously described (*27, 83*). All experimental mice were obtained from timed matings of $HEB^{fl/fl}$ x $HEB^{fl/fl}$ Vav-iCre, which gave rise WT and HEB-deleted littermates, differing only in the presence of Cre. Id3 deficient mice (Id3-KO) lacked Id3 in all cells due to a knock-in of RFP into the *Id3* locus resulting in a knock-in/knock-out allele (JAX strain # 010983, B6;129S-*Id3*$^{tm1Pzg}$/J**)**. RFP was

quenched by intracellular staining. Id3-KO mice were bred onto the C57Bl/6 background for 8 generations. Id3$^{+/-}$ mice were mated together to produce WT and Id3-KO littermates. Adult mice were analyzed at 6-8 weeks of age. Mice were bred and maintained in the Comparative Research Facility of the Sunnybrook Research Institute (Toronto, Ontario, Canada) under specific pathogen-free conditions. All animal procedures were approved by the Sunnybrook Research Institute Animal Care Committee.

**Timed Matings and Embryo Harvest**

Timed matings were performed by setting up mating pairs (day 0) and separating them ~16 hrs later. Embryos were harvested 18 days later. Fetal thymuses were dissected out of embryos and single cell suspensions were generated by mechanical disruption and filtered through 40-micron mesh. Cells were resuspended in PBS for sorting or flow cytometry. Embryos were processed and analyzed separately, and tail tissue was collected for genotyping and sample identification.

**Flow cytometry**

Antibodies were purchased from eBiosciences (San Diego, California, USA), Biolegend (San Diego, California, USA) and BD Biosciences (Mississauga, Ontario, Canada). The 5′ libraries using to generate the HEB cKO scRNA-seq data directly detected *Tcrg-V6* mRNA, whereas the 3′ libraries did not permit detection of *Tcrg-V* or *Trdv* transcripts. For flow cytometry, cells were washed and incubated with Fc blocking antibody (BD Biosciences), followed by extracellular staining for surface CD4 (clone GK1.5), CD8α (clone 53–6.7), CD3 (clone 145-2C11), TCRγδ (clone GL3), TCRβ (clone H57–597), Vγ4 (Vγ2; clone UC3-10A6), Vγ5 (Vγ3; clone 536), Vγ1 (Vγ1.1; clone 2.11), CD27 (clone LG3-1A10), Vδ6.3 (clone 8F4H7B7, CD24 (clone M1/ 69), CD73 (clone TY11.8), CD44 (clone IM7), CD25 (clone PC615). To assess functional capacities, cells were stimulated by incubation for five h with PMA (50 ng/ml) and Ionomycin (500 ng/ml)

in the presence of Brefeldin A (5mg/ml; eBioscience), washed with 1XHBSS/BSA, and incubated with Fc block before staining for surface epitopes. Cells were then fixed and permeabilized (Fix and Perm Cell Permeabilization Kit; eBioscience) and stained with antibodies against IL-17A (clone eBio17B7). For intracellular transcription factor staining, the cells were fixed, permeabilized (FoxP3 Staining Kit, eBioscience) and stained for RORγt (clone B2D), MAF (clone sym0F1), and PLZF (clone R17-809). All flow cytometric analyses were performed using Becton-Dickenson (BD) LSRII, Fortessa, or SymphonyA5-SE. FACSDiva and FlowJo software were used for analysis. Sorting was performed on BD ARIA and BD Fusion sorters.

**Single-cell RNA sequencing**

E18 fetal thymuses from HEB cKO mice were dissected from embryos and individually pushed through a 40-micron mesh with a syringe plunger. Cells were incubated with Fc block for 30 min on ice. Small aliquots from each sample were stained with CD4, CD8, and CD3 to assess the genotypes, with a lack of DP indicating HEB deletion. Genotypes were verified by PCR. The remainder of the cells (3 WT and 3 HEB cKO) were stained and sorted for TCR$\gamma\delta^+$CD3$^+$ cells. Single cells were isolated using the 10X Chromium controller and barcoded libraries were generated using the Chromium Next GEM Single Cell 5' Kit v2 (Dual Index) (10X Genomics) at the Princess Margaret Genomics Facility (Toronto, ON, Canada). Next generation Illumina sequencing was performed to a depth of ~20,000 reads.

E18 fetal thymuses from Id3-KO mice were dissected from embryos, pushed through mesh as above, and incubated with Fc block. Embryos were genotyped by PCR, and thymocytes were pooled according to genotype. DN (CD4$^-$CD8$^-$) cells were enriched by magnetic sorting using anti-CD4 and anti-CD8 microbeads according to manufacturer's instructions (Miltenyi Biotech). Flow

through cells were processed in-house as above but using the Chromium Next GEM Single Cell 3' Kit v2 (Dual Index) (10X Genomics).

**scRNA-seq data analysis**

FASTQ raw data files were aligned to the mm10 genome using Cell Ranger version 1.1.7 (10X Genomics) (*84*). Matrix files were analyzed using programs in R Seurat version 4.4 (*85*), as detailed in the R-Markdown file (supplementary material). WT and HEBcKO datasets were processed for quality control by excluding cells with more than 7% mitochondrial genes and less than 1000 genes or 4000 RNA sequences, resulting in 1272 WT cells and 1951 HEB cKO cells for further analysis. Filtered WT and HEB cKO datasets were merged, and SCTransform was applied to the merged dataset to limit the variation due to sequencing depth. Cell cycle regression was performed to mitigate the influence of cell cycle heterogeneity on clustering. Cells expressing high levels of *Lyz2* were excluded to remove most myeloid cells. PCA analysis was performed (RunPCA) and used to compute a nearest neighbor graph (FindNeighbors) and identify clusters (FindClusters). UMAP plots were generated using RunUMAP, and displayed using DimPlot_scCustom. FindMarkers was used to generate heatmaps (DoHeatmap) of the top ten genes most differentially expressed (DEGs) between the clusters. Since the DEGs in cluster 8 indicated a myeloid identity, this cluster was removed, and the remaining cells were re-clustered. UMAP plots were generated showing 1) clusters in the merged dataset and 2) distribution of WT versus HEBcKO cells within each cluster, 3) WT cells only, and 4) HEBcKO cells only. The re-clustered merged dataset was used to generate a heatmap using DoHeatmap, which aided in assigning cluster identities. To further evaluate cluster identity, we generated curated gene sets based on the literature (*24, 65, 76, 86, 87*) and used them to create module scores corresponding to αβ and γδ T cell developmental subsets. Importantly, module scores were based on the inclusion

of all genes in the gene set used to specify the module. Module scores were compared among merged clusters using Stacked_VlnPlot, and split feature plots were used to display the localization and intensity of module scoring in the UMAP clusters. Comparisons of the expression of single genes between WT and HEBcKO clusters was shown using split feature plots and split violin plots. A clustered dot plot of genes diagnostic for αβ and γδ T cell subsets was generated for the merged dataset to further assist in cluster identification. To compare cluster 1, composed mostly of HEBcKO cells, and cluster 4, composed mostly of WT cells, in the merged dataset, we performed FindMarkers using the Wilcox test, minimum three cells per feature and three cells per group. The Enhanced Volcano Plot was calculated with a pCutoff = 10e-26, and an FCcutoff = 0.5.

For the Id3-KO dataset, the following analysis was conducted. FASTQ raw data files were aligned to the mm39 genome using Cell Ranger. R-Seurat programs were used to filter the cells as described above in the HEB cKO dataset, resulting in 2324 WT cells and 2895 cells for further analysis. Datasets were merged and subjected to SCTransform as above. PCA plots were generated and used to construct UMAP plots depicting clusters in merged datasets and distribution of WT versus Id3-KO cells across the UMAP. Feature plots and violin plots were used to identify clusters with γδ T cell characteristics. Clusters 6 and 9 were subsetted, and new clusters were obtained using FindClusters. A myeloid cluster was omitted, and a split UMAP were generated to show localization of WT versus HEB cKO cells. Violin plots were generated to classify the four remaining clusters, and split violin plots were generated to show relative expression of early and late γδ T cell genes in WT versus HEB cKO cells within each cluster.

**Gene module curation**

Genes included in each module were chosen as described above. The genes chosen for each module are as follows: DN3 (*Il2ra*, *Ptcra*, *Rag1*, *Cd24a*), DP (*Rag1*, *Cd8a*, *Cd8b1*), early γδ T cell precursors (γδTe: *Il17re, Cd24a, Blk, Maf, Sox13, Etv5, Ccr9, Sox4, Igfbp4, Rora, Rorc, Cpa3, Il17a, Gzma, Sell, Sox5*), immature γδT17 cells (γδT17 imm: *Il17re, Blk, Maf, Ccr9, Rorc, Nr4a1, Il21r, Sox13, Id3*), mature γδT17 cells (γδT17 mat: *Il17re, Blk, Maf, Rorc, Il23r, Cxcr6, Il1r1, Zbtb16*), immature γδT1 cells (γδT1 imm: *Il2rb, Cd24a, Nr4a1, Xcl1, Il21r, Id3*) and mature γδT1 cells (γδT1 mat: *Il2rb, Fcer1g, Klrd1, Klra5, Tyrobp, Ifitm1, Xcl1, Cxcr3, Zbtb16, Id3*) subsets. Co-expression of all genes included in the module was required for cells to be assigned a positive module score.

**Supplemental Information**

**Supplementary Figure 1**. Defects in αβ T cell development in fetal thymus of HEB cKO mice.

**Supplementary Figure 2**. Alterations in gene expression in fetal γδ T cells of HEB cKO mice.

**Supplementary Figure 3**. Profound expansion of Vγ1 Vδ6.3 γδ T cells in Id3-KO adult thymus.

**Supplementary Figure 4**. Normal αβ T cell development in Id3-KO fetal thymus.

**Acknowledgments.** We would like to thank Lisa Wells, Madeline Harvey, Vivien Musiime, and the SRI Animal Facility for excellent mouse care. We thank Yuan Zhuang for provision of the HEB cKO and Id3-KO mice. We are thankful to David Wiest for thoughtful discussions and providing valuable insights. We are indebted to the SickKids Flow Cytometry Core (supported by the Canadian Foundation for Innovation (CFI) and the SickKids' Foundation) for antibody panel design and high parameter flow cytometry analysis, and the SRI Flow Cytometry and Microscopy Core for flow cytometry and sorting. We also thank the UHN Princess Margaret Genomics Facility for construction of the WT and HEBcKO scRNA-seq libraries. The Digital Research Alliance of Canada (RRG #5070) provided cloud computing capacity for scRNA-seq data analysis.

**Funding.** This work was supported by the Canadian Institutes for Health Research (CIHR; PJT 153058 to MKA, FDN154332 and PJT192050 to JCZP**,** and PJT165973 to CJG), National Institutes of Health (NIH: 1P01AI102853-06) to MKA and JCZP, and a CFI John Evans Fund Leaders' Infrastructure Grant to CJG (#37562). JS was supported by an American Association for Immunologists Careers in Immunology Award and a CIHR Postdoctoral Fellowship. VR was supported by a CIHR Postdoctoral Fellowship, and HW was the recipient of an Ontario Graduate Scholarship.

**Author contributions.** J.S.S. and M.K.A. conceptualized the study. E.S.R., M.S.G, and C.J.G. developed high parameter flow cytometry panels. J.S.S., E.S.R., and J.D.R. collected the flow cytometry data, and J.S.S. sorted cells for the scRNA-seq experiments. M.K.A. analyzed the scRNA-seq data, assisted by H.W. and V.R., and generated the figures. V.R. and H.W.

performed the *Id3* scRNA-seq experiment. Funding was acquired by M.K.A. and J.C.Z.P. M.K.A., J.C.Z.P., and C.M. interpreted the data and formed the model. M.K.A. wrote the first draft of the manuscript, and all authors contributed to the final manuscript.

**Conflict of Interest**

The authors declare there are no conflicts of interest.

**Data and materials availability.** Matrix files and R-markdown code have been deposited to the Dryad repository and can be accessed private for review at:

HEB-WT scRNA-seq matrix files and R-markdown code

https://doi.org/10.5061/dryad.08kprr5cq

HEB cKO scRNA-seq matrix files and R-markdown code

https://doi.org/10.5061/dryad.qv9s4mwqh

Id3-WT scRNA-seq matrix files and R-markdown code

https://doi.org/10.5061/dryad.j6q573nqd

Id3-KO scRNA-seq matrix files and R-markdown code

https://doi.org/10.5061/dryad.x0k6djhvj

## REFERENCES


1. S. Itohara *et al.*, Homing of a gamma delta thymocyte subset with homogeneous T-cell receptors to mucosal epithelia. *Nature* **343**, 754-757 (1990).
2. A. H. Hovav, A. Wilharm, O. Barel, I. Prinz, Development and Function of gammadeltaT Cells in the Oral Mucosa. *J Dent Res* **99**, 498-505 (2020).
3. L. Monin *et al.*, gammadelta T cells compose a developmentally regulated intrauterine population and protect against vaginal candidiasis. *Mucosal Immunol*, (2020).
4. A. Akitsu, Y. Iwakura, Interleukin-17-producing gammadelta T (gammadelta17) cells in inflammatory diseases. *Immunology* **155**, 418-426 (2018).
5. D. Kadekar *et al.*, The neonatal microenvironment programs innate gammadelta T cells through the transcription factor STAT5. *J Clin Invest* **130**, 2496-2508 (2020).
6. K. Alves de Lima *et al.*, Meningeal gammadelta T cells regulate anxiety-like behavior via IL-17a signaling in neurons. *Nat Immunol* **21**, 1421-1429 (2020).
7. D. Wakita *et al.*, Tumor-infiltrating IL-17-producing gammadelta T cells support the progression of tumor by promoting angiogenesis. *Eur J Immunol* **40**, 1927-1937 (2010).
8. S. B. Coffelt *et al.*, IL-17-producing gammadelta T cells and neutrophils conspire to promote breast cancer metastasis. *Nature* **522**, 345-348 (2015).
9. A. C. Kohlgruber *et al.*, gammadelta T cells producing interleukin-17A regulate adipose regulatory T cell homeostasis and thermogenesis. *Nat Immunol* **19**, 464-474 (2018).
10. S. P. Fahl, D. J. Kappes, D. L. Wiest, in *Signaling Mechanisms Regulating T Cell Diversity and Function,* J. Soboloff, D. J. Kappes, Eds. (Boca Raton (FL), 2018), pp. 85-104.
11. M. H. Sieweke, T. Graf, A transcription factor party during blood cell differentiation. *Curr Opin Genet Dev* **8**, 545-551 (1998).
12. M. M. Karimi *et al.*, The order and logic of CD4 versus CD8 lineage choice and differentiation in mouse thymus. *Nat Commun* **12**, 99 (2021).

13. I. Gimferrer *et al.*, Regulation of GATA-3 expression during CD4 lineage differentiation. *J Immunol* **186**, 3892-3898 (2011).

14. I. Taniuchi, Views on helper/cytotoxic lineage choice from a bottom-up approach. *Immunol Rev* **271**, 98-113 (2016).

15. H. K. Komori *et al.*, Cutting edge: dendritic epidermal gammadelta T cell ligands are rapidly and locally expressed by keratinocytes following cutaneous wounding. *J Immunol* **188**, 2972-2976 (2012).

16. M. Girardi *et al.*, Regulation of cutaneous malignancy by gammadelta T cells. *Science* **294**, 605-609 (2001).

17. Y. S. Chen *et al.*, IL-17-producing gammadelta T cells protect against Clostridium difficile infection. *J Clin Invest* **130**, 2377-2390 (2020).

18. M. D. Johnson, D. A. Witherden, W. L. Havran, The Role of Tissue-resident T Cells in Stress Surveillance and Tissue Maintenance. *Cells* **9**, (2020).

19. N. Schmolka *et al.*, Epigenetic and transcriptional signatures of stable versus plastic differentiation of proinflammatory gammadelta T cell subsets. *Nat Immunol* **14**, 1093-1100 (2013).

20. Y. H. Chien, X. Zeng, I. Prinz, The natural and the inducible: interleukin (IL)-17-producing gammadelta T cells. *Trends Immunol* **34**, 151-154 (2013).

21. K. Joannou *et al.*, γδ Thymocyte Maturation and Emigration in Adult Mice. *J Immunol* **208**, 2131-2140 (2022).

22. D. J. Gerber *et al.*, IL-4-producing gamma delta T cells that express a very restricted TCR repertoire are preferentially localized in liver and spleen. *J Immunol* **163**, 3076-3082 (1999).

23. V. Azuara, J. P. Levraud, M. P. Lembezat, P. Pereira, A novel subset of adult gamma delta thymocytes that secretes a distinct pattern of cytokines and expresses a very restricted T cell receptor repertoire. *Eur J Immunol* **27**, 544-553 (1997).

24. A. du Halgouet *et al.*, Multimodal profiling reveals site-specific adaptation and tissue residency hallmarks of gammadelta T cells across organs in mice. *Nat Immunol* **25**, 343-356 (2024).

25. M. M. Nielsen, D. A. Witherden, W. L. Havran, gammadelta T cells in homeostasis and host defence of epithelial barrier tissues. *Nat Rev Immunol* **17**, 733-745 (2017).

26. F. Lambolez *et al.*, Characterization of T cell differentiation in the murine gut. *J Exp Med* **195**, 437-449 (2002).

27. T. S. H. In *et al.*, HEB is required for the specification of fetal IL-17-producing gammadelta T cells. *Nat Commun* **8**, 2004 (2017).

28. E. Kashani *et al.*, A clonotypic Vgamma4Jgamma1/Vdelta5Ddelta2Jdelta1 innate gammadelta T-cell population restricted to the CCR6(+)CD27(-) subset. *Nat Commun* **6**, 6477 (2015).

29. I. Sandrock *et al.*, Genetic models reveal origin, persistence and non-redundant functions of IL-17-producing gammadelta T cells. *J Exp Med* **215**, 3006-3018 (2018).

30. W. L. Havran, J. P. Allison, Developmentally ordered appearance of thymocytes expressing different T-cell antigen receptors. *Nature* **335**, 443-445 (1988).

31. S. R. Carding, P. J. Egan, Gammadelta T cells: functional plasticity and heterogeneity. *Nat Rev Immunol* **2**, 336-345 (2002).

32. N. Xiong, L. Zhang, C. Kang, D. H. Raulet, Gene placement and competition control T cell receptor gamma variable region gene rearrangement. *J Exp Med* **205**, 929-938 (2008).

33. J. S. Heilig, S. Tonegawa, Diversity of murine gamma genes and expression in fetal and adult T lymphocytes. *Nature* **322**, 836-840 (1986).

34. K. L. Edelblum *et al.*, gammadelta Intraepithelial Lymphocyte Migration Limits Transepithelial Pathogen Invasion and Systemic Disease in Mice. *Gastroenterology* **148**, 1417-1426 (2015).

35. B. Blom *et al.*, Disruption of alpha beta but not of gamma delta T cell development by overexpression of the helix-loop-helix protein Id3 in committed T cell progenitors. *EMBO J* **18**, 2793-2802 (1999).

36. L. Tan *et al.*, A fetal wave of human type 3 effector gammadelta cells with restricted TCR diversity persists into adulthood. *Sci Immunol* **6**, (2021).

37. G. Sanchez Sanchez, Y. Tafesse, M. Papadopoulou, D. Vermijlen, Surfing on the waves of the human γδ T cell ontogenic sea. *Immunol Rev* **315**, 89-107 (2023).

38. M. K. Anderson, J. D. B. da Rocha, Direct regulation of TCR rearrangement and expression by E proteins during early T cell development. *WIREs Mech Dis*, e1578 (2022).

39. M. K. Anderson, J. S. Selvaratnam, Interaction between gammadeltaTCR signaling and the E protein-Id axis in gammadelta T cell development. *Immunol Rev* **298**, 181-197 (2020).

40. M. Munoz-Ruiz *et al.*, TCR signal strength controls thymic differentiation of discrete proinflammatory gammadelta T cell subsets. *Nat Immunol* **17**, 721-727 (2016).

41. E. L. Y. Chen *et al.*, Ontogenic timing, T cell receptor signal strength, and Notch signaling direct γδ T cell functional differentiation in vivo. *Cell Rep* **35**, 109227 (2021).

42. S. Scaramuzzino *et al.*, Single-cell transcriptomics uncovers an instructive T-cell receptor role in adult gammadelta T-cell lineage commitment. *EMBO J* **41**, e110023 (2022).

43. M. C. Haks *et al.*, Attenuation of gammadeltaTCR signaling efficiently diverts thymocytes to the alphabeta lineage. *Immunity* **22**, 595-606 (2005).

44. S. M. Hayes, L. Li, P. E. Love, TCR signal strength influences alphabeta/gammadelta lineage fate. *Immunity* **22**, 583-593 (2005).

45. S. Y. Lee, J. Stadanlick, D. J. Kappes, D. L. Wiest, Towards a molecular understanding of the differential signals regulating alphabeta/gammadelta T lineage choice. *Semin Immunol* **22**, 237-246 (2010).

46. N. Sumaria, S. Martin, D. J. Pennington, Constrained TCRgammadelta-associated Syk activity engages PI3K to facilitate thymic development of IL-17A-secreting gammadelta T cells. *Sci Signal* **14**, (2021).

47. G. Turchinovich, A. C. Hayday, Skint-1 identifies a common molecular mechanism for the development of interferon-gamma-secreting versus interleukin-17-secreting gammadelta T cells. *Immunity* **35**, 59-68 (2011).

48. P. Zarin *et al.*, Integration of T-cell receptor, Notch and cytokine signals programs mouse gammadelta T-cell effector differentiation. *Immunol Cell Biol* **96**, 994-1007 (2018).

49. F. Coffey *et al.*, The TCR ligand-inducible expression of CD73 marks gammadelta lineage commitment and a metastable intermediate in effector specification. *J Exp Med* **211**, 329-343 (2014).

50. M. Munoz-Ruiz, N. Sumaria, D. J. Pennington, B. Silva-Santos, Thymic Determinants of gammadelta T Cell Differentiation. *Trends Immunol* **38**, 336-344 (2017).

51. N. A. Spidale *et al.*, Interleukin-17-Producing gammadelta T Cells Originate from SOX13(+) Progenitors that Are Independent of gammadeltaTCR Signaling. *Immunity* **49**, 857-872 e855 (2018).

52. S. P. Fahl *et al.*, The E protein-TCF1 axis controls gammadelta T cell development and effector fate. *Cell Rep* **34**, 108716 (2021).

53. T. Ikawa, H. Kawamoto, A. W. Goldrath, C. Murre, E proteins and Notch signaling cooperate to promote T cell lineage specification and commitment. *J Exp Med* **203**, 1329-1342 (2006).

54. H. Xi, R. Schwartz, I. Engel, C. Murre, G. J. Kersh, Interplay between RORgammat, Egr3, and E proteins controls proliferation in response to pre-TCR signals. *Immunity* **24**, 813-826 (2006).

55. M. E. Jones-Mason *et al.*, E protein transcription factors are required for the development of CD4(+) lineage T cells. *Immunity* **36**, 348-361 (2012).

56. C. Murre, Helix-loop-helix proteins and the advent of cellular diversity: 30 years of discovery. *Genes Dev* **33**, 6-25 (2019).

57. G. Bain *et al.*, Regulation of the helix-loop-helix proteins, E2A and Id3, by the Ras-ERK MAPK cascade. *Nat Immunol* **2**, 165-171 (2001).

58. I. Engel, C. Johns, G. Bain, R. R. Rivera, C. Murre, Early thymocyte development is regulated by modulation of E2A protein activity. *J Exp Med* **194**, 733-745 (2001).

59. J. P. Lauritsen *et al.*, Marked induction of the helix-loop-helix protein Id3 promotes the gammadelta T cell fate and renders their functional maturation Notch independent. *Immunity* **31**, 565-575 (2009).

60. E. S. Alonzo *et al.*, Development of promyelocytic zinc finger and ThPOK-expressing innate gamma delta T cells is controlled by strength of TCR signaling and Id3. *J Immunol* **184**, 1268-1279 (2010).

61. X. Han *et al.*, E-protein regulatory network links TCR signaling to effector Treg cell differentiation. *Proc Natl Acad Sci U S A*, (2019).

62. R. Barndt, M. F. Dai, Y. Zhuang, A novel role for HEB downstream or parallel to the pre-TCR signaling pathway during alpha beta thymopoiesis. *J Immunol* **163**, 3331-3343 (1999).

63. J. Wojciechowski, A. Lai, M. Kondo, Y. Zhuang, E2A and HEB are required to block thymocyte proliferation prior to pre-TCR expression. *J Immunol* **178**, 5717-5726 (2007).

64. C. Paget *et al.*, CD3bright signals on gammadelta T cells identify IL-17A-producing Vgamma6Vdelta1+ T cells. *Immunol Cell Biol* **93**, 198-212 (2015).

65. Sagar *et al.*, Deciphering the regulatory landscape of fetal and adult γδ T-cell development at single-cell resolution. *Embo j* **39**, e104159 (2020).

66. K. Narayan *et al.*, Intrathymic programming of effector fates in three molecularly distinct gammadelta T cell subtypes. *Nat Immunol* **13**, 511-518 (2012).

67. A. E. Moran *et al.*, T cell receptor signal strength in Treg and iNKT cell development demonstrated by a novel fluorescent reporter mouse. *J Exp Med* **208**, 1279-1289 (2011).

68. B. Zhang, A. Jiao, M. Dai, D. L. Wiest, Y. Zhuang, Id3 Restricts gammadelta NKT Cell Expansion by Controlling Egr2 and c-Myc Activity. *J Immunol* **201**, 1452-1459 (2018).

69. M. Verykokakis *et al.*, Inhibitor of DNA binding 3 limits development of murine slam-associated adaptor protein-dependent "innate" gammadelta T cells. *PLoS One* **5**, e9303 (2010).

70. I. Ueda-Hayakawa, J. Mahlios, Y. Zhuang, Id3 restricts the developmental potential of gamma delta lineage during thymopoiesis. *J Immunol* **182**, 5306-5316 (2009).

71. B. Zhang, Y. Y. Lin, M. Dai, Y. Zhuang, Id3 and Id2 act as a dual safety mechanism in regulating the development and population size of innate-like gammadelta T cells. *J Immunol* **192**, 1055-1063 (2014).

72. N. Sumaria, C. L. Grandjean, B. Silva-Santos, D. J. Pennington, Strong TCRgammadelta Signaling Prohibits Thymic Development of IL-17A-Secreting gammadelta T Cells. *Cell Rep* **19**, 2469-2476 (2017).

73. G. Bain, W. J. Romanow, K. Albers, W. L. Havran, C. Murre, Positive and negative regulation of V(D)J recombination by the E2A proteins. *J Exp Med* **189**, 289-300 (1999).

74. M. Nozaki *et al.*, Regulation of TCR Vgamma2 gene rearrangement by the helix-loop-helix protein, E2A. *Int Immunol* **23**, 297-305 (2011).

75. A. Mihai *et al.*, E proteins control the development of NKgammadeltaT cells through their invariant T cell receptor. *Nat Commun* **15**, 5078 (2024).

76. O. Dienz *et al.*, Critical Role for SLAM/SAP Signaling in the Thymic Developmental Programming of IL-17- and IFN-gamma-Producing gammadelta T Cells. *J Immunol* **204**, 1521-1534 (2020).

77. M. L. Michel *et al.*, Interleukin 7 (IL-7) selectively promotes mouse and human IL-17-producing gammadelta cells. *Proc Natl Acad Sci U S A* **109**, 17549-17554 (2012).

78. J. C. Ribot *et al.*, CD27 is a thymic determinant of the balance between interferon-gamma- and interleukin 17-producing gammadelta T cell subsets. *Nat Immunol* **10**, 427-436 (2009).

79. K. Yoganathan *et al.*, Regulation of the Signal-Dependent E Protein HEBAlt Through a YYY Motif Is Required for Progression Through T Cell Development. *Front Immunol* **13**, 848577 (2022).

80. S. J. Yoon, J. W. Foley, J. C. Baker, HEB associates with PRC2 and SMAD2/3 to regulate developmental fates. *Nat Commun* **6**, 6546 (2015).

81. J. de Boer *et al.*, Transgenic mice with hematopoietic and lymphoid specific expression of Cre. *Eur J Immunol* **33**, 314-325 (2003).

82. S. Siegemund, J. Shepherd, C. Xiao, K. Sauer, hCD2-iCre and Vav-iCre mediated gene recombination patterns in murine hematopoietic cells. *PLoS One* **10**, e0124661 (2015).

83. E. Welinder *et al.*, The transcription factors E2A and HEB act in concert to induce the expression of FOXO1 in the common lymphoid progenitor. *Proc Natl Acad Sci U S A* **108**, 17402-17407 (2011).

84. G. X. Zheng *et al.*, Massively parallel digital transcriptional profiling of single cells. *Nat Commun* **8**, 14049 (2017).

85. Y. Hao *et al.*, Integrated analysis of multimodal single-cell data. *Cell* **184**, 3573-3587 e3529 (2021).

86. M. K. Zuberbuehler *et al.*, The transcription factor c-Maf is essential for the commitment of IL-17-producing gammadelta T cells. *Nat Immunol* **20**, 73-85 (2019).

87. T. S. Heng, M. W. Painter, C. Immunological Genome Project, The Immunological Genome Project: networks of gene expression in immune cells. *Nat Immunol* **9**, 1091-1094 (2008).

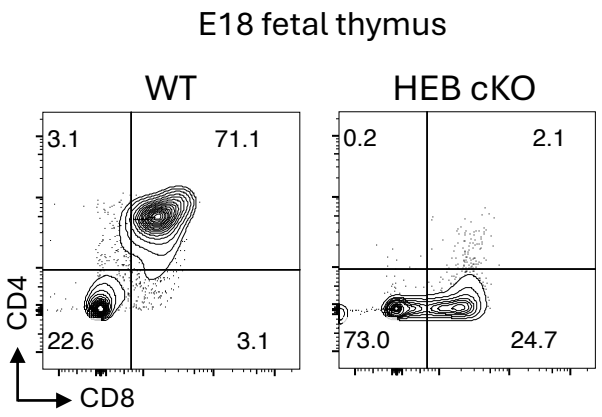


Supplementary Figure 1. Defects in αβ T cell development in fetal thymus of HEB cKO mice. Thymocytes were dissected from E18 WT (HEB fl/fl; left) and HEB cKO (right) littermates and subjected to flow cytometry. At E18 very few cells have become CD4 or CD8 single positives with most cells at the DP stage in WT mice. The DN to DP transition is severely arrested in HEB cKO fetal thymus, like the adult thymus phenotype.

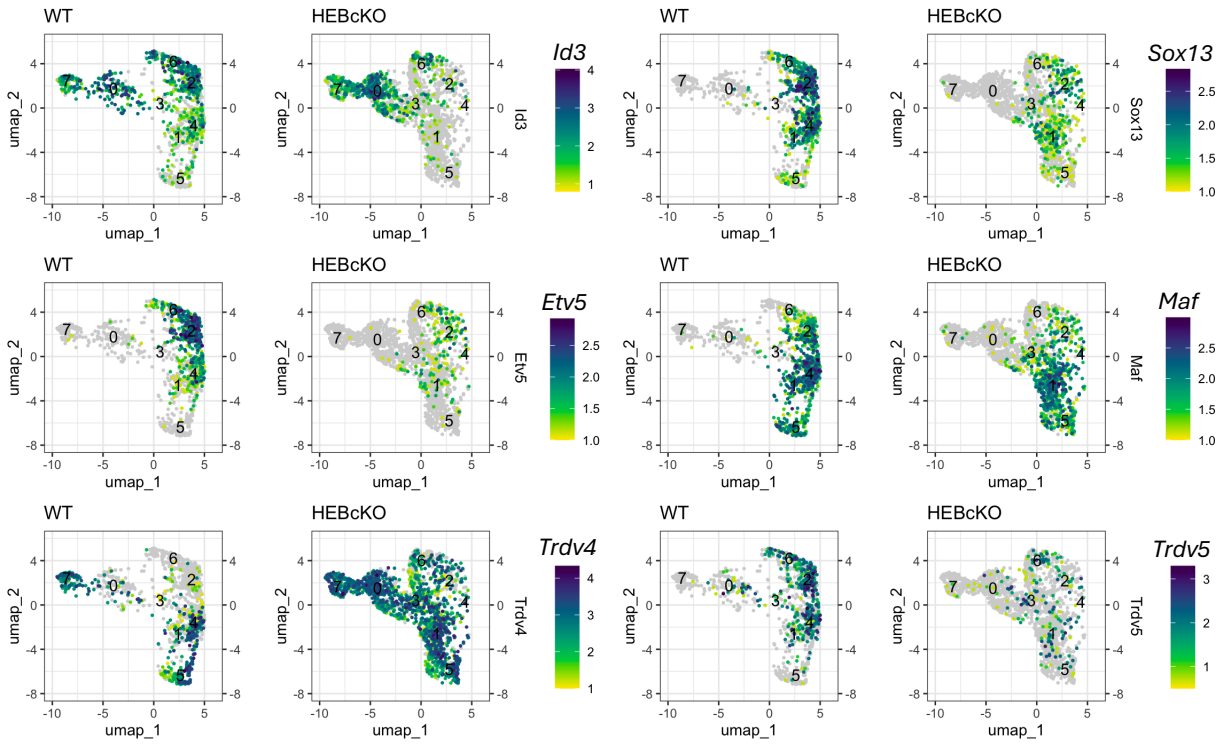


Supplementary Figure 2. Alterations in gene expression in fetal γδ T cells of HEB cKO mice. E18 fetal thymocytes were dissected from WT (HEB fl/fl; left) and HEB cKO (right) littermates, followed by sorting of γδ T cells and scRNA-seq. Split feature plots were generated to examine the distribution of transcripts for individual genes (identified to the right over the scales) in WT (left) and HEB cKO (right) γδ T cell populations.

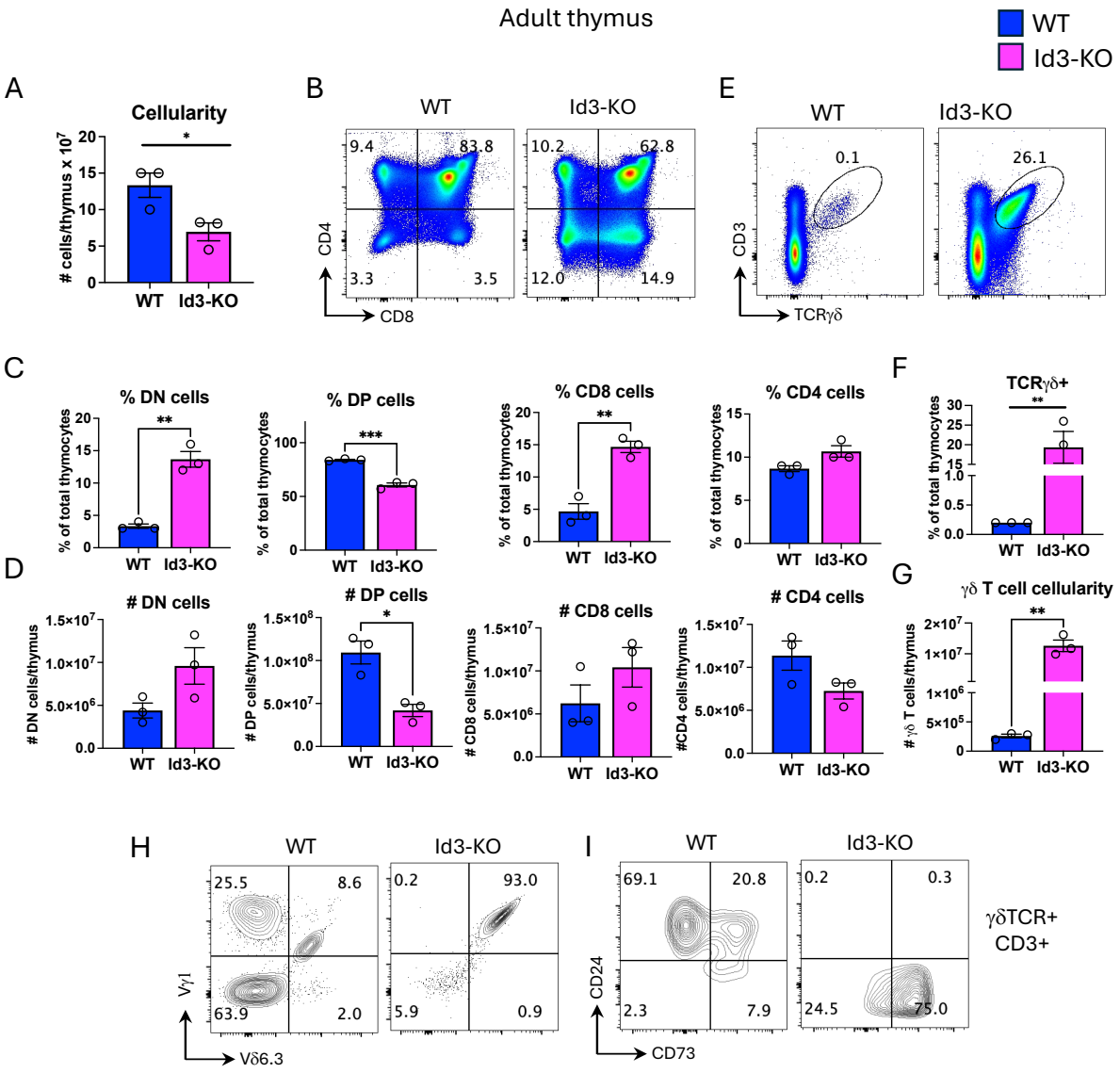


Supplementary Figure 3. Profound expansion of Vγ1 Vδ6.3 γδ T cells in Id3-KO adult thymus. Adult thymocytes from WT and Id3-KO littermates were analyzed by flow cytometry. A. Total cellularity of WT versus Id3-KO thymus. B. Flow cytometry plots of CD4 and CD8 expression. C. Percentages of thymocyte developmental subsets. D. Absolute cell numbers per thymus of thymocyte developmental subsets. E. Flow cytometry plots of γδ T cells. F. Percentage of γδ T cells. G. Absolute cell numbers of γδ T cells per thymus. H. Flow cytometry plots of percentages of Vγ1/Vδ6.3 subsets in γδ T cells. I. Flow cytometry plots of CD24+CD73- (immature), CD24+CD73- (committed), and CD24-CD73- (mature) γδ T cells WT = blue, Id3-KO = pink. All flow plots were gated on live lymphocytes except (H) and (I) which were gated on γδTCR+CD3+ cells.

E18 thymus

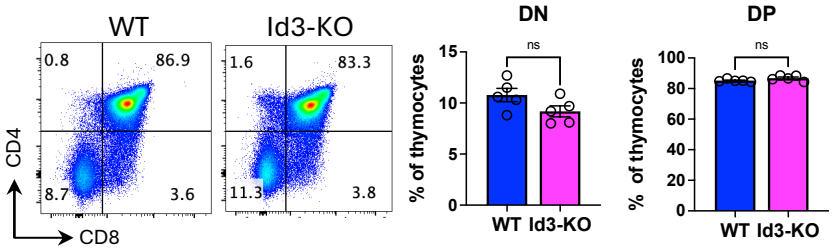


Supplementary Figure 4. Normal αβ T cell development in Id3-KO fetal thymus. E18 thymocytes were dissected from WT and Id3-KO (right) littermates and analyzed by flow cytometry. At E18 very few cells have become CD4 or CD8 single positives with most cells at the DP (CD4+CD8+; double positive) stage. DN (CD4-CD8-; double negative) and DP percentages are unperturbed, and overall thymic cellularity is unchanged (see Fig. 4A) between WT and Id3-KO fetal thymus. WT=blue, Id3-KO=pink.